Sliding Grafted Polymer Layers

Vladimir A. Baulin,[†] **Albert Johner,**[‡,†] **and Carlos M. Marques**[*,†,‡]

Centre de Recherche Macromoléculaires, Institut Charles Sadron, 67083 Strasbourg Cedex, France, and Laboratoire Européen Associé, ICS (Strasbourg)/MPIP (Mainz) Ackermannweg 10, 55128 Mainz, Germany

ABSTRACT: We study theoretically the structure of sliding grafted polymer layers, or SGP layers. These interfacial structures are built by attaching each polymer to the substrate with a ringlike molecule such as cyclodextrins. Such a topological grafting mode allows the chains to freely slide along the attachment point. Escape from the sliding link is prevented by bulky capping groups. We show that grafts in the mushroom regime adopt mainly symmetric configurations (with comparable branch sizes), while grafts in dense layers are highly dissymmetric so that only one branch *per* graft participates in the layer. Sliding layers on small colloids or starlike sliding micelles exhibit an intermediate behavior, where the number of longer branches participating in the corona is independent of the total number of branches. This regime also exists for sliding surface micelles comprising less chains, but it is narrower.

1. Introduction

Rotaxanes are molecular complexes formed when a ringlike molecule, the rotor, is threaded over a linear molecule, the rotating axis.[1] The polymeric versions of rotaxanes are named polyrotaxanes. These necklace structures are built by threading several ring molecules over a polymer chain. Unthreading is also prevented by subsequent capping of the chain ends.[2,3] Although the usual chemical and physical forces are also at work in polyrotaxanes, the peculiar character of these complexes is determined by the topological nature of each of its components. Such materials are thus also known as topological materials. Polyrotaxanes are being intensely scrutinized for advanced specific applications as molecular shuttles, "insulated molecular wires", supramolecular light-harvesting antenna systems, or sliding gels.[4−9] They can be made from different linear polymers[10,11] combined with different cyclic molecules in different solvents.[12] One of the most well-studied systems involves poly(ethylene oxide) and cyclodextrins, which are oligosaccharides of six, seven, or eight glucose units assembled as rings. Although in most cases polyrotaxanes are formed with a very high density of cyclodextrins threaded over the polymer chain, recent strategies for complex formation[13] allow for only one or a low number of cyclodextrins per chain. The cyclodextrin can then further be grafted to a surface, resulting in a grafted polymer layer where the chains retain the ability to slide through the grafting ring. We coin the acronym SGP layers for such structures, standing for sliding grafted polymer layers.

Layers of grafted polymers have a wide range of applications,[14] ranging from the colloidal stabilization of industry formulations, water treatment, and mineral recovery, to the control of surface wetting and adhesion or the protection of stealth liposomes from the human immune system in drug delivery.[15] Sparsely grafted polymers are often referred to as mushrooms, while more dense systems above the surface overlapping density are known as brushes. Polymer theories for mushrooms and brushes have been developed during the past two decades,[16−19] and their predictions successfully compared with elegant experiments.[20] In this paper, we revisit grafted polymer theories introducing a key modification that will allow the polymer to be attached to the surface in a sliding manner. As we shall see, this induces important differences in the equilibrium and dynamic behavior of the layers, both in the mushroom and brush regimes. In section 2, we consider ideal sliding mushrooms of chains grafted with one or several sliding links. Section 3 discusses denser layers, and the crossover from sliding mushrooms to sliding brushes is discussed in section 4. In section 5, we account for excluded volume correlations and focus on sliding bulk and surface aggregates that embody the sliding mushroom as a special case. The final section reviews our key results and discusses their experimental relevance.

2. SGP Layers: Mushroom Regime

We study here SGP layers composed of isolated chains grafted to a planar surface by a sliding link. We assume Gaussian statistics and will discuss later in section 5 excluded volume effects.

2.1. Fixed Sliding Links. The sliding link is attached to a fixed position on the surface and allows free exchange of monomers between the two branches of the chain with the total number of monomers N, see Figure 1. Thus, one branch has n monomers, the other branch has $N - n$ monomers. The Gaussian nature of the two branches results in the absence of branch correlations and the Green function[21] of a chain is the product of the Green functions of the two branches. Let the grafting point be at $\mathbf{a} = \{0,0,a\}$, where a is a monomer size. The total Green function reads

$$G(\mathbf{r},\mathbf{r}') = G_n(\mathbf{r},\mathbf{a})G_{N-n}(\mathbf{a},\mathbf{r}') \qquad (1)$$

where $\mathbf{r}$ and $\mathbf{r}'$ are the coordinates of free ends. The Green functions factorize over the directions x, y, and z, i.e. $G_n(\mathbf{r},\mathbf{r}') = G_n^x(x,x')G_n^y(y,y')G_n^z(z,z')$. In the x and y directions, the Green functions retain then bulk structure: $G_n^x(x,x') = (3/2\pi na^2))^{1/2} \exp[(-3/2)(na^2)(x - x')^2]$,

* Author to whom correspondence should be addressed. E-mail: marques@fresnel.u-strasbg.fr.
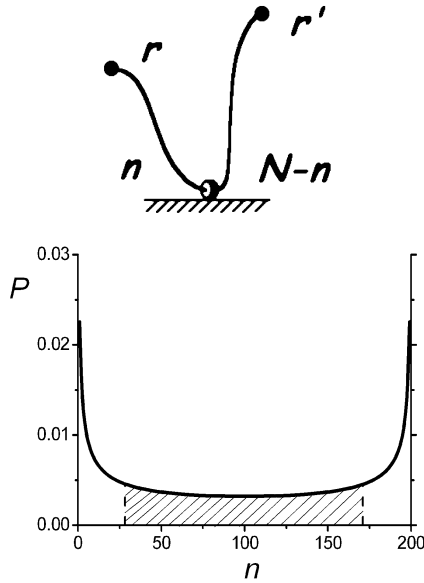† Institut Charles Sadron.
‡ Laboratoire Européen Associé.

Figure 1. Schematic picture and the lengths distribution function of a Gaussian chain grafted to a surface by a sliding link. Two branches can exchange monomers, while the total chain length is fixed $N = 200$. The central region which corresponds to symmetric configurations is defined by the condition $\int_n^{N-n} P(n)\, dn = 1/2$ (hatched).

and for a similar term for $G_n^z(z,z')$ within the z direction, one needs to account for the impermeability of the wall:

$$G_n^z(z,z') = \left(\frac{3}{2\pi na^2}\right)^{1/2}\left[\exp\left(-\frac{3}{2na^2}(z-z')^2\right) - \exp\left(-\frac{3}{2na^2}(z+z')^2\right)\right] \quad (2)$$

We focus first on the probability distribution function $P(n)$ describing the number of configurations with branches of length n and $N - n$. The probability distribution $P(n)$ is calculated from the partition function $Z(n) = \int G(\mathbf{r},\mathbf{r}')\, d\mathbf{r}\, d\mathbf{r}'$, as $P(n) = Z(n)/Z$, with $Z = \int_0^N Z(n)\, dn$. In the limit where the radius of gyration of each branch is larger then a monomer size, i.e. $R_g(n) \sim a\sqrt{n} \gg a$, $P(n)$ can be written as

$$P(n) = \frac{1}{\pi\sqrt{n(N-n)}} \quad (3)$$

The equivalence of the two branches is reflected in the symmetry of this function, which has a minimum at $n = N/2$. This partition function is dominated by *symmetric* configurations in the sense that it presents only a weak divergence at $n = 0$ which does not dominate its integral. Half of the branches (Figure 1) belong to the central region $1/2 - \sqrt{2}/4 < n/N < 1/2 + \sqrt{2}/4$.

We consider now a Gaussian chain grafted to a plane surface by *two* fixed sliding links at a distance D between them. The position of two grafting points are $\mathbf{a}_1 = \{0,0,a\}$ and $\mathbf{a}_2 = \{D,0,a\}$. The chain has two free ends comprising n_1 and n_3 monomers and one middle loop with n_2 monomers, while the total number of monomers in the chain is $N = n_1 + n_2 + n_3$. The Green function of the chain is

$$G(\mathbf{r},\mathbf{r}') = G_{n_1}(\mathbf{r},\mathbf{a}_1)G_{n_2}(\mathbf{a}_1,\mathbf{a}_2)G_{n_3}(\mathbf{a}_2,\mathbf{r}') \quad (4)$$
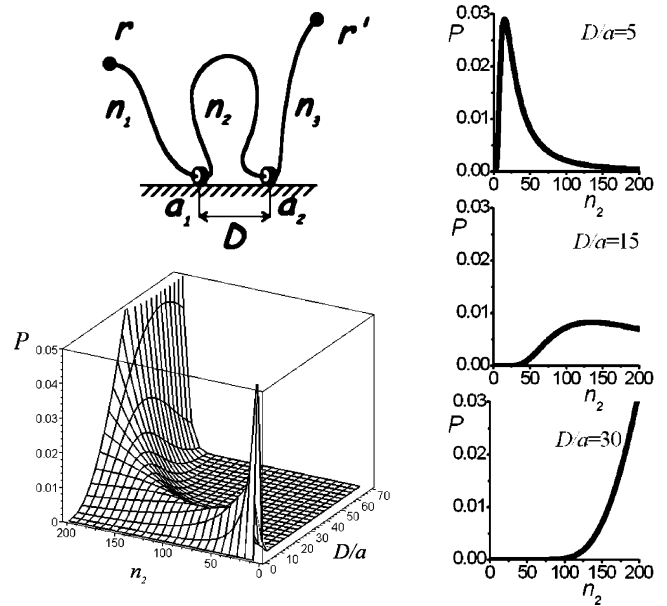

Figure 2. Polymer chain grafted to a surface by two sliding links $\mathbf{a}_1$ and $\mathbf{a}_2$ separated by the distance D between them and the distribution of monomers in the loop $P(n_2)$ for the total chain length $N = 200$. The 2D cuts for $D/a = 5$, 15, and 30 are shown in the inset.

The integration over positions of the free ends, $\mathbf{r}$ and $\mathbf{r}'$, gives as before the partition function for the tails and now also for the loop. It can be expressed for instance as a function of the number of monomers in the first tail, n_1, and the number of monomers in the loop, n_2:

$$Z(n_1,n_2) \sim \frac{1}{\sqrt{n_1(N-n_1-n_2)}}\frac{\exp\left[-\frac{3D^2}{2n_2}\right]}{n_2^{3/2}}(1 - e^{-6/n_2}) \quad (5)$$

The first term expresses the usual free end contribution of the form $n^{-1/2}$, while the last two terms account for the loop. Since the two free ends are identical, we concentrate on the probability distribution for the monomers in the loop $P(n_2) = Z(n_2)/Z$, where the loop partition function $Z(n_2) = \int_0^{N-n_2} Z(n_1,n_2)\, dn_1$ is given by

$$Z(n_2) = \pi\frac{\exp\left[-\frac{3D^2}{2n_2}\right]}{n_2^{3/2}}(1 - e^{-6/n_2}) \quad (6)$$

and the total partition function is $Z = \int_0^N Z(n_2)\, dn_2$. A three-dimensional plot of $P(n_2)$ is presented in Figure 2. If the distance D between the links is large, most of the monomers are in the loop and the sliding chain behaves as a chain fixed by two ends. For small distances, a loop is entropically unfavorable and the monomers are distributed between the two ends. If the chain is grafted by three grafting points (Figure 3), the two loops turn out to be identical and the monomers are distributed equally between them. Thus, for a single loop, the number of monomers in the loop corresponding to the maximum of $P(n_2)$ goes to N for large D, while for two loops, it tends to $N/2$. This implies the emergence of two loops of equal size (Figure 4). In the general case of a chain grafted by m sliding links separated by the
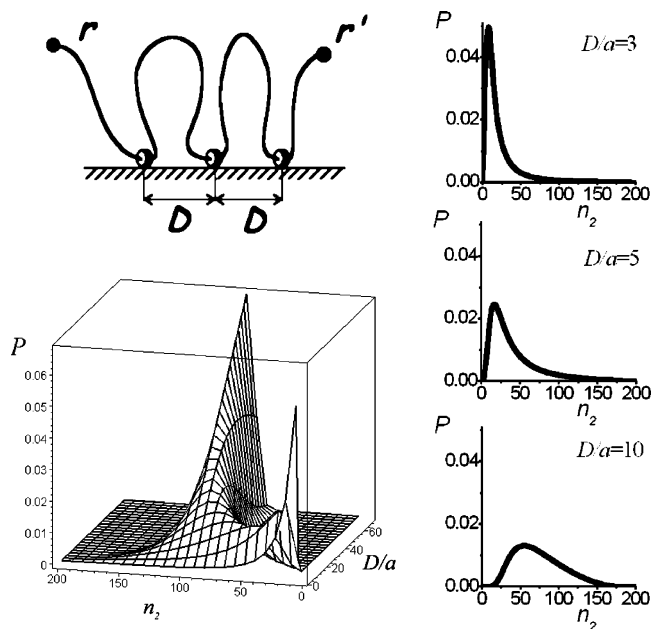
Figure 3. Polymer chain grafted by three sliding links with a distance D between them and the distribution of monomers in one of the loops $P(n_2)$ for the total chain length $N = 200$. The 2D cuts for $D/a = 3$, 5, and 10 are shown in the inset.
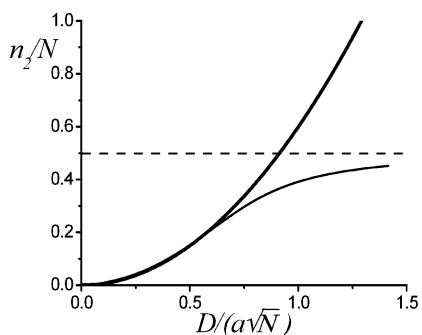

Figure 4. Fraction of monomers in the loop n_2/N corresponding to the maximum of the distribution $P(n_2)$ as a function of a scaled distance between the grafting points $D/(a\sqrt{N})$ for a chain grafted by *two* (thick) and *three* (thin) sliding links. Compare with Figures 2 and 3.

distances $D_1, D_2, ..., D_{m-1}$ along the x direction such that $n_k \gg 1$, the partition function is the product

$$Z(n_1, n_2, ..., n_{m+1}) \sim \frac{1}{\sqrt{n_1 n_{m+1}}} \prod_{k=2}^{m} \frac{\exp\left(-\dfrac{3(D_{k-1}/a)^2}{2n_k}\right)}{n_k^{5/2}} \quad (7)$$

which is completed by the condition of conservation of monomers $N = \sum_{k=1}^{m+1} n_k$. Since the total partition function is the convolution integral over all variables, it can be calculated by Laplace transform.[22] This allows us to calculate the long chain limit of the total partition function

$$Z_{N \to \infty} \sim \prod_{k=2}^{m} \frac{1}{(D_{k-1}/a)^3} \quad (8)$$

The structure of eq 7 suggests that different loops are equivalent to each other. In particular, if the distances
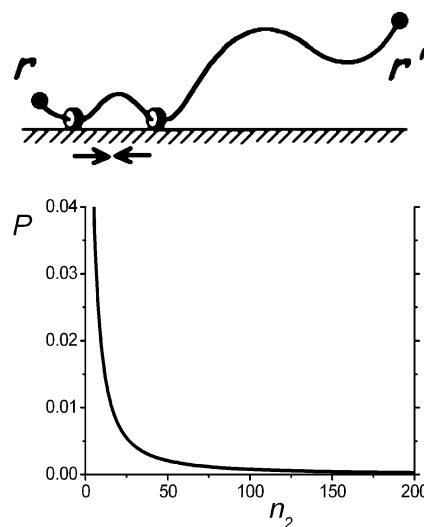
between grafting points are equal, $D_{k-1} = D$, the monomers should be equally distributed between the loops.

2.2. Sliding Links with Lateral Mobility. Let us turn to the situation where not only the chain can slide through the grafting points but the grafting points themselves can freely move on the surface. This can be the case when cyclodextrins are grafted to the surface of a liquid membrane. If a chain is grafted by a single mobile link, the redistribution of monomers between two branches is the same as in the case of a fixed grafting point (Figure 1). However, in the case of several mobile grafting points, the distribution of monomers between free ends and loops is changed.

Consider *two* mobile sliding links placed at $\mathbf{a}_1 = \{x_1, y_1, a\}$ and $\mathbf{a}_2 = \{x_2, y_2, a\}$. We can use again the expression of the Green function for fixed grafting points (eq 4), but now the partition function is obtained by the integration both on positions of free ends and positions of sliding links: $Z(n_1, n_2) = \int G(r, r') \, d\mathbf{r} \, d\mathbf{r}' \, d\mathbf{a}_1 \, d\mathbf{a}_2$

$$Z(n_1, n_2) = \frac{1}{\sqrt{n_1 n_2 (N - n_1 - n_2)}} (1 - e^{-6/n_2}) \quad (9)$$

Integration over the tails n_1 gives the distribution function of monomers in the loop

$$P(n_2) = \frac{1}{Z} \frac{\pi}{n_2^{3/2}}, \quad (n_2 > 1) \quad (10)$$

where $Z = \int_0^N Z(n_2) \, dn_2$ is the total partition function. $P(n_2)$ is presented in Figure 5. It rapidly decreases with the increasing size of the loop n_2, which shows that large loops are not favorable. In general, when a sliding chain is grafted by several mobile sliding links, the system acquires two additional degrees of freedom (two transversal coordinates). Each of them contributes to the partition function as $\sqrt{n_k}$. Thus,

$$Z(n_1, n_2, ..., n_{m+1}) \sim \frac{1}{\sqrt{n_1 n_{m+1}}} \prod_{k=2}^{m} \frac{1}{n_k^{3/2}} \quad (11)$$
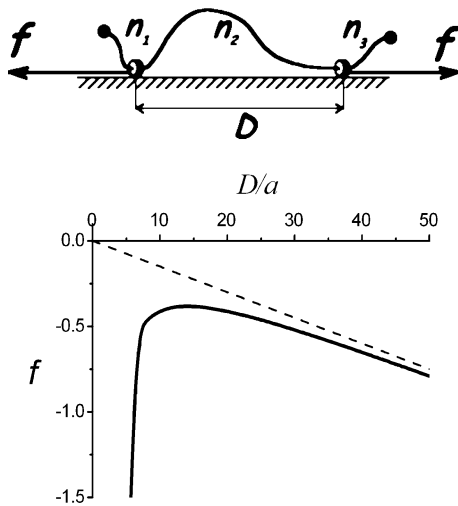
Applying the Laplace transform to the total partition

Figure 5. Chain grafted by freely moving sliding links and corresponding distribution of monomers in a loop $P(n_2)$ for $N = 200$.

Figure 6. Extension force, f, of a chain grafted by two sliding links as a function of a distance D between them (solid) in comparison to the extension of the end-grafted Gaussian chain of the same length (dash). The total chain length is $N = 200$.

Figure 7. Transversal dimension of a *sliding chain* $\langle R_x \rangle/\sqrt{Na^2/6}$ as a function of the scaled force $\beta = \sqrt{Na^2/6}$ applied to a free end (solid) in comparison with the dimension of the *end-grafted chain* of the same length N (dash dot) and two times shorter chain $N/2$ (dash).

function we get $Z \sim (1/\sqrt{N})^{(m-1)}$. The form of the partition function brings us to the same conclusion: the system prefers to eliminate the loops. This leads to an effective entropic attraction between mobile grafts, which tend to stick together even in the absence of any additional forces.

2.3. Sliding Grafted Chain under a Pulling Force. Once the sliding links are stuck together, one needs to apply the force to separate them. In Figure 6, we plot the force in units of kT needed to separate the two links to the distance D: $f = \partial \ln Z/\partial D$. At large distances, $D^2/(Na^2) \gg 1$, the force coincides with that of the chain grafted by two ends, $f = -3D/(Na)$. At small distances, $D^2/(Na^2) \ll 1$, the curve has a logarithmic divergence, $f \sim \ln(D/a)$. The curve passes by a maximum coinciding with the creation of the loop.

We can see the difference between a chain grafted by one end to a surface and a chain grafted by a sliding link also when one applies a force parallel to the surface to one of free ends $\mathbf{f} = \{f_x, 0, 0\}$. The partition function of a sliding grafted chain under a pulling force is

$$Z(\mathbf{r}') = \int_0^N dn \int d\mathbf{r} \, G_n(\mathbf{r}, \mathbf{a}) G_{N-n}(\mathbf{a}, \mathbf{r}') e^{f_x r_x'} \quad (12)$$

and the total partition function $Z = \int Z(\mathbf{r}') \, d\mathbf{r}'$ is

$$Z = 6e^{\beta/2} I_0(\beta/2) \quad (13)$$

where $\beta = (Na^2/6)f_x^2$ is a scaling parameter associated with the magnitude of the applied force $\mathbf{f}$ and $I_0(x)$ is the zero-order Bessel I function.[23] At the same time, the corresponding partition functions of an end-grafted chain, denoted by the subscript 0, are $Z_0(\mathbf{r}') = G_N(\mathbf{a}, \mathbf{r}') e^{f_x r_x'}$ and $Z_0 \sim e^{\beta}/\sqrt{N}$ for large N.

For a relatively large force, f_x, both end-grafted and sliding chains are fully stretched with comparable configurations. However, for relatively small f_x, a sliding chain prefers symmetric configurations with two branches of more or less equal size. In this limit, the sliding chains resemble two end-grafted chains comprised of $N/2$ monomers. To illustrate such behavior, we compare the average distance from the grafting point in the x direction for both chains. The average distance
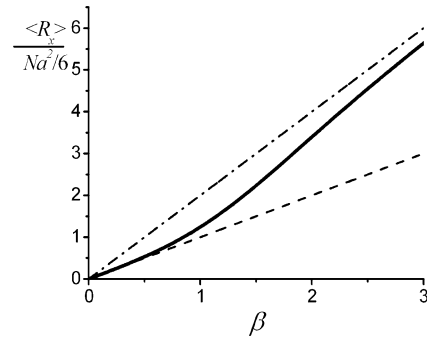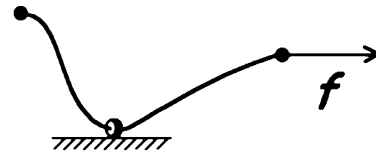
for an end-grafted chain is $\langle R_x \rangle_0 = (Na^2/3)f_x$, while the average distance for a sliding chain is

$$\langle R_x \rangle = \frac{\langle R_x \rangle_0}{2}\left(1 + \frac{I_1\left(\frac{\beta}{2}\right)}{I_0\left(\frac{\beta}{2}\right)}\right) \quad (14)$$

The resulting curves are plotted in Figure 7. The increasing force provokes the transition of a sliding chain from a symmetric configuration with two branches of size $N/2$ to fully stretched with a single branch of length N.

The same behavior is expected for the average square distance from the grafting point. In the case of an end-grafted chain, we obtain $\langle R_x^2 \rangle_0 = (Na^2/3)(1 + 2\beta)$, while for a sliding chain

$$\langle R_x^2 \rangle = \frac{\langle R_x^2 \rangle_0}{2}\left(1 - \frac{1 - 2\beta}{1 + 2\beta}\frac{I_1\left(\frac{\beta}{2}\right)}{I_0\left(\frac{\beta}{2}\right)}\right) \quad (15)$$

A sliding chain has more degrees of freedom as compared to an end-tethered chain. The *dispersion* of the size

$$\Delta(\beta) = \sqrt{\frac{\langle R_x^2 \rangle - \langle R_x \rangle^2}{\langle R_x^2 \rangle}} \quad (16)$$

of the chain under a pulling force is larger than that of the end-grafted chain of the same length (Figure 8). As expected, the dispersion of a sliding chain coincides with the dispersion of an end-grafted chain when the chains are very stretched.

3. SGP Layers: Brush Regime

When the grafting density in the SGP layers is high enough, the different chains and chain branches will interact strongly. Each chain can exchange monomers between two branches. Although lengths of individual chains are equal, lengths of their branches can vary
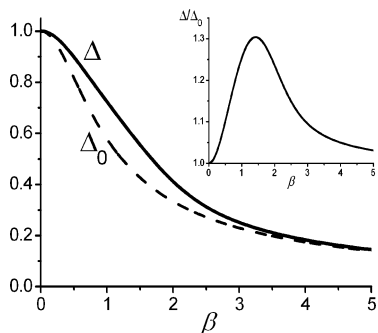
Figure 8. The dispersion $\Delta = \sqrt{(\langle R_x^2 \rangle - \langle R_x \rangle^2)/\langle R_x^2 \rangle}$ of a sliding chain (solid) and an end-grafted chain, Δ_0, of the same length (dash) under a pulling force applied to a free end. Inset: the relation, Δ/Δ_0, between dispersions of sliding and end-grafted chains.

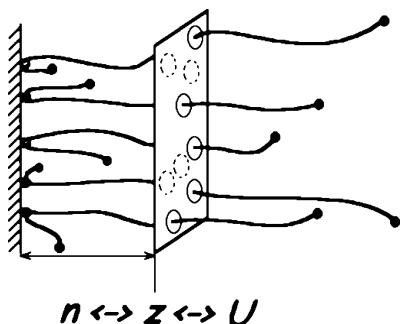$$n \leftrightarrow z \leftrightarrow U$$

Figure 9. Schematic picture of a brush of sliding polymers.

from chain to chain. Hence, one can assume that the branches of the sliding chains are independent "chains" of annealed length composing a brush with annealed polydispersity (Figure 9). We will treat a polydisperse brush in the framework of the self-consistent field theory of brushes in the strong stretching regime[19] valid for high grafting densities. In this limit, the configurations of chains are considered as trajectories, $z(n)$, of effective "particles" moving in the field U which depends only on the distance from the grafting surface. Thus, the molecular weight of a chain n is analogous to the time needed for a "particle" for traveling from any distance z_0 to the grafting surface $z = 0$. This analogy leads to a Newton equation of motion for $z(n)$, the distance from the grafting surface

$$\frac{d^2 z}{dn^2} = \frac{dU}{dz} \tag{17}$$

This allows to relate the distance, z, the molecular weight of a chain, n, and the self-consistent potential, U. We consider all three variables to be dimensionless.

Let $\sigma(n)$ be the number of chains per unit area with molecular weight n. Then, $S(n) = \int_n^N \sigma(n) \, dn$ is the number per unit area of chains with molecular weight larger than n. The total number of chains per unit area is $S_0 \equiv S(n = 0)$. The polydispersity, $\sigma(n)$, is related to the distribution of chain lengths, $P(n)$. Thus, we can write $S(n) = S_0 \int_n^N P(n) \, dn$, where $P(n)$ is normalized: $\int_0^N P(n) \, dn = 1$. This expression can be rewritten as

$$S(n) = S_0 \int_z^H P(z) \, dz = S_0 \int_0^U P(U') \, dU' \tag{18}$$

The concentration at a given height z (or potential U) is constructed by chains whose ends start at larger heights z' (lower potentials $U' < U$):

$$\phi(z(U)) = S_0 \int_0^U P(U') \frac{dn}{dz}(U,U') \, dU' =$$
$$S_0 \int_0^U \frac{P(U') \, dU'}{\sqrt{2(U - U')}} \tag{19}$$

Here, the expression for dz/dn is obtained from the integration of eq 17.

We will write the potential U in the form $U = (w^2/2)\phi^2$, which corresponds to a θ solution, where the mean field approximation is justified. Here, w^2 is the effective third virial coefficient. This form will allow us to get analytical results, which remain qualitatively correct also for a more conventional choice assuming two-body interactions (good solvent). We can eliminate the volume fraction, ϕ, and write eq 19 as a closed equation for $P(U')$:

$$\frac{\sqrt{2}}{w}\sqrt{U} = S_0 \int_0^U \frac{P(U') \, dU'}{\sqrt{2(U - U')}} \tag{20}$$

The solution of this equation, obtained using the Laplace transform[24] is

$$U(n) = wS(n) \tag{21}$$

The chemical potential of a chain is a sum of the chemical potentials of the two branches $\mu_{\text{chain}} = [\mu(n) + \mu(N - n)]/2$ where $\mu(n) = \int_0^N U(n') \, dn'$. We can write $\mu_{\text{chain}}(n)$ as a functional of $P(n)$ which we integrate by parts using the symmetry of $P(n)$

$$\mu_{\text{chain}} = \frac{wS_0}{2}[\int_0^n dn' \int_{n'}^N P(n'') \, dn'' +$$
$$\int_0^{N-n} dn' \int_{n'}^N P(n'') \, dn''] = \frac{wS_0}{2}[\int_0^n (N - n +$$
$$n')P(n') \, dn' + \int_n^N (N - n' + n)P(n') \, dn'] \tag{22}$$

Minimization of the free energy functional

$$F\{P(n)\} = \frac{S_0{}^2}{2} \int_0^N P(n)\mu_{\text{chain}}\{P(n)\} \, dn \tag{23}$$

with respect to $P(n)$ along with the normalization condition $\int_0^N P(n) \, dn = 1$ gives the equilibrium distribution of chain lengths:

$$P(n) = \begin{cases} \frac{1}{2} \delta(n) & 0 < n < \frac{N}{2} \\ \frac{1}{2} \delta(N - n) & \frac{N}{2} < n < N \end{cases} \tag{24}$$

In a densely grafted layer, the chains adopt very dissymmetric configurations and behave as end-grafted chains. The strong stretching approximation ignores local density fluctuations in the layer. We expect the δ functions in eq 24 to stand for localized functions decaying over one correlation length (*blob* size). This we consider next.

4. Transition from Sliding Mushrooms to Sliding Brushes

As we have seen, a single Gaussian chain grafted by a sliding link prefers symmetric configurations, while
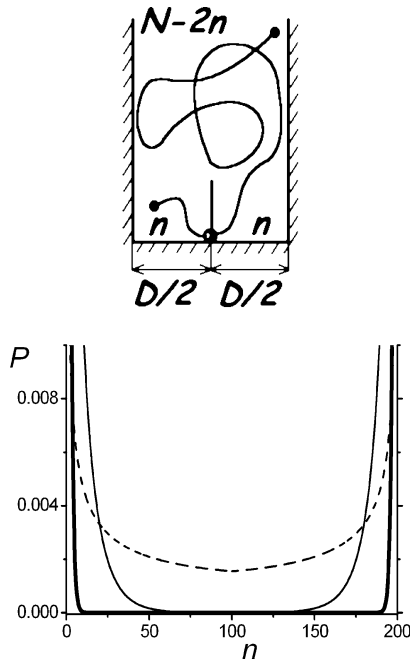
Figure 10. Lengths distribution function of a sliding chain in a box for $N = 200$ and the wall-to-wall distance $D/a = 80$ (dash), $D/a = 15$ (thin), and $D/a = 5$ (thick).

sliding chains in a densely grafted brush adopt stretched asymmetric configurations. Thus, there must be a crossover region between the two configurations as the grafting density is increased. Such an intermediate situation can be modeled as a Gaussian chain in a box. The walls of the box mimic the steric repulsion of neighboring chains and the decreasing distance between the walls models the increasing grafting density. To model the steric repulsion between two branches of the same chain, we place a wall with a height equal to the size of the shortest branch in the middle of the box as depicted in Figure 10. Assume that the shortest branch has n monomers and the distance between the walls is D. The shortest branch and the part of the longest branch of length n are confined in smaller boxes of width $D/2$, while the rest of the longest branch of length $N - 2n$ is in the box of width D.

Such intermediate regime corresponds to $Na^2 > D^2$ and $na^2 < D^2$. In these limits, the partition function of the chain confined in the box is

$$Z = Z_{\parallel}^4\left(n, \frac{D}{2}\right) Z_{\parallel}^2(N - 2n, D) Z_{\perp}(n, a) Z_{\perp}(N - n, a) \quad (25)$$

where the perpendicular component is

$$Z_{\perp}(n, a) = \mathrm{erf}\left(\sqrt{\frac{3}{2n}}\right) \sim \frac{1}{\sqrt{n}} \quad (26)$$

and the component parallel to the grafting surface is[21]

$$Z_{\parallel}\left(n, \frac{D}{2}\right) = \frac{4}{\pi} \sum_{p=1}^{\infty} \frac{1}{p} \sin^3\left(\frac{\pi p}{2}\right) \exp\left(-\frac{\pi^2 p^2 n a^2}{6D^2}\right) \quad (27)$$

Since $na^2 < D^2$, we can approximate this expression by the first mode

$$Z_{\parallel}\left(n, \frac{D}{2}\right) \sim \exp\left(-\frac{\pi^2 n a^2}{6D^2}\right) \quad (28)$$

Thus, the partition function has the form

$$Z \sim \frac{\exp\left(-\dfrac{2\pi^2 n a^2}{D^2}\right)}{\sqrt{n(N - n)}} \quad (29)$$

which is valid for n corresponding to the short branch. Normalization of this function leads to the following expression for the distribution of the ends

$$P(n) = \frac{1}{2\pi I_0\left(\pi^2 \dfrac{Na^2}{D^2}\right)} \times$$

$$\frac{1}{\sqrt{n(N - n)}}\begin{cases} \exp\left(2\pi^2 \dfrac{\left(\dfrac{N}{2} - n\right)a^2}{D^2}\right) & 0 < n < \dfrac{N}{2} \\[4mm] \exp\left(2\pi^2 \dfrac{\left(n - \dfrac{N}{2}\right)a^2}{D^2}\right) & \dfrac{N}{2} < n < N \end{cases} \quad (30)$$

In the limit $Na^2 \gg D^2$ and $na^2 \ll D^2$, this function can be approximated by

$$P(n) \sim \frac{a}{D} \frac{1}{\sqrt{n}} \quad (31)$$

This gives the estimate of the crossover value for the length the shorter branch: $\sqrt{n^*} \sim D/a$. Above the overlap grafting density, the size distribution of the branches is bimodal, the shorter branch comprising of order D^2/a^2 monomers counts one *blob*. When the overlap density is approached from above, the size distribution spreads over the whole interval and more symmetric configurations are favored (Figure 10).

5. SGP Layers in Curved Geometries: Stars and Micelles

We consider now the case where the sliding links that anchor the polymer are attached to curved surfaces, with radii much smaller than the unperturbed chain size. This might be the case, for instance, if cyclodextrin rings are attached on a packed configuration, resulting in a starlike polymer. More commonly, this would also be the result of the micellization of amphiphilic molecules carrying cyclodextrins as the headgroups. In any of these cases, the resulting starlike object is composed of a fixed number of arms with annealed lengths. Notice that such a bulk configuration can also arise at interfaces if ring association takes place close to an impenetrable wall. In this section, we first describe the partition function of the usual three-dimensional star and adapt such description for the annealed case; we then extend our results to the case of a surface star.

The partition function Z_p of a star[25] with p equal branches of contour length N is given by the critical exponent γ_p, $Z_p = N^{\gamma_p - 1}$. Because a two arm star is also a linear chain, one must have $\gamma_1 = \gamma_2$.

Let us now consider a star with two arms of length n_1 and $n_2 > n_1$, the partition function obeys the general scaling form $n_1^{\gamma_2 - 1}(n_2/n_1)^x$. In the limiting case $n_1 \sim 1$, the one arm partition function should be recovered, hence $x = \gamma_1 - 1$. This is now generalized to an arbitrary star.[26]

For a star with polydispersed arms all of different sizes, ranging from the smallest, n_l, to the largest, n_p, the partition function can be constructed step by step. Let first all p arms have the size n_1, the partition function is $n_1^{\gamma_p-1}$, let now all chains but one grow to the next size n_2, the partition function becomes $n_1^{\gamma_p-1}n_2^{\gamma_{p-1}-1}/n_1^{\gamma_{p-1}-1}$; in the next step, let all outer chains but one grow to the next size n_3 and so on. As a result:

$$Z_p = n_1^{\gamma_p-\gamma_{p-1}}n_2^{\gamma_{p-1}-\gamma_{p-2}} \dots n_{p-1}^{0}n_p^{\gamma_1-1} \qquad (32)$$

Consider now a sliding aggregate comprising q chains. Let us characterize each chain by the smallest of its two arms, the largest being its complement to N, and let n_l be the smallest of these q arms, all by definition smaller than $N/2$. The partition function of the sliding aggregate reads:

$$Z(q) = \int_{cut}^{N/2} dn_q n_q^{\gamma_{q+1}-\gamma_q}(N -$$
$$n_q)^{\gamma_q-\gamma_{q-1}} \dots \int_{cut}^{n_2} dn_1 n_1^{\gamma_{2q}-\gamma_{2q-1}}(N - n_1)^{\gamma_1-1} \quad (33)$$

The behavior of $Z(q)$ depends on whether the integrals are dominated by the upper or the lower boundary, the lower boundary being a monomeric cut-off length. Let p^* be the value of the index such as $\gamma_{p^*} - \gamma_{p^*-1} > -1$ and $\gamma_{p^*+1} - \gamma_{p^*} \leq -1$.

(i) If there are few chains *per* aggregate ($2q \leq p^*$), all integrals are dominated by the upper boundary and hence by symmetric configurations.

$$Z(q) \propto N^q N^{\gamma_{2q}-1} \qquad (34)$$

This corresponds to a $2q$-arm star, the extra factor stands for the choice of monomers located at the core.

(ii) In the opposite limit of many chains *per* aggregate ($q \geq p^*$), all integrals are dominated by the lower boundary and hence by very dissymmetric chain configurations.

$$Z(q) \propto N^{\gamma_q-1} \qquad (35)$$

This corresponds to a q-arm star.

(iii) In the intermediate regime ($q < p^* < 2q$), there are essentially $2q - p^*$ dissymmetric chains and hence $p^* - q$ symmetric ones. The aggregate is thus equivalent to a p^* star with an additional factor accounting for the freedom of symmetric configurations.

$$Z(q) \propto N^{p^*-q} N^{\gamma_{p^*}-1} \qquad (36)$$

Star exponents, γ_p, are known exactly in two dimensions and for ideal chains ($d > 4$). Otherwise first-order ϵ expansions ($\epsilon = 4 - d$) are available.[25]

$$\gamma_p - 1 = (4 + 9p(3 - p))/64 \quad d = 2 \text{ (exact)}$$

$$\gamma_p - 1 = 0 \quad d > 4 \text{ (exact)}$$

$$\gamma_p - 1 = \frac{\epsilon}{16}p(3 - p) + o(\epsilon^2) \quad d = 4 - \epsilon$$
$$(37)$$

These estimates allow for an exact determination of p^* in two dimensions; we get $p^* = 5$, the first-order ϵ expansion happens to give the same value. Assuming that the first-order ϵ expansions also give a fair estimate of p^* in three dimensions, we obtain $p^* = 9$. The intermediate regime where only part of the chains are
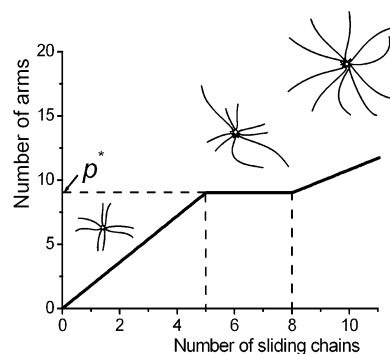

Figure 11. Number of arms, p, of a sliding bulk star as a function of the number of sliding chains, q. For a sliding surface star, only the crossover values are changed.

dissymmetric hence extends over aggregation numbers 5 to 8. Like the flat brush limit, the Daoud and Cotton limit ($p \gg 1$, $\gamma_p \propto p^{d/(d-1)}$) is dominated by dissymmetric configurations (Figure 11).

Similar arguments can be developed for sliding surface aggregates with a small core grafted on an impenetrable wall. The critical exponents, γ_p, have to be replaced by the corresponding surface exponents γ_p^s in eqs 32−36. The following estimates of the surface exponents can be used:[25]

$$\gamma_p^s - 1 = p(15 - 18p)/64 \quad d = 2 \text{ (exact)}$$

$$\gamma_p^s - 1 = -p/2 \quad d > 4 \text{ (exact)}$$

$$\gamma_p^s - 1 = -p/2 + \frac{\epsilon}{16}p(3 - p) + o(\epsilon^2) \quad d = 4 - \epsilon$$
$$(38)$$

The first-order ϵ expansion gives the estimate $p^{*s} = 3$ in two dimensions and $p^{*s} = 5$ in three dimensions. The former is to be compared with the exact value $p^{*s} = 2$ in two dimensions. The first-order ϵ expansion is likely to slightly overestimate p^{*s} also in three dimensions. If one would use the Daoud and Cotton[27]-like approximation, $\gamma_p^s/\gamma_{2p} = 1/2$, which is exact for infinite p, one would get $p^{*s} = p^*/2$. As expected, excluded volume correlations are stronger at the surface and favor dissymmetric configurations. In three dimensions, the intermediate regime is narrow and covers aggregation numbers 3 and 4 on the basis of the above estimates.

This discussion embodies the special case $p = 1$ of a single chain described in the ideal case earlier. Let again n be the length of the shorter branch, following eq 32, with surface exponents, we can write the partition function

$$Z(n) = (N - n)^{\gamma_1^s-1}n^{\gamma_1-\gamma_1^s-1} \quad n < N \qquad (39)$$

where the exact relation $\gamma_2^s = \gamma_1 - 1$ between critical exponents has been used. Equation 3 is recovered, up to the unimportant normalization factor if ideal exponents are inserted. At first order in ϵ, $\gamma_1 - \gamma_1^s = 1/2 + o(\epsilon^2)$, a quadratic interpolation between $d = 2$ and $d = 4$ gives the estimate $\gamma_1 - \gamma_1^s = 1/2 - 0.027$; the weak divergence of $Z(n)$ at $n = 0$ is only slightly stronger than in the ideal case. Sliding grafts on small colloids or sliding starlike micelles illustrate thus the interesting adaptability of sliding grafted chains. If there are only a few chains *per* colloid or micelle, they adopt symmetric configurations and hence all branches participate in the

corona. If there are many chains *per* colloid or micelle, they adopt highly dissymmetric configurations and only half of the branches participate in the corona. Interestingly, there is an intermediate regime where a fixed number, p^*, of branches participates in the corona. This suggests that in this regime fluctuations in the number of grafts, or aggregation number, could be somehow washed out. Following our estimate based on critical exponents, aggregates comprising from five to eight chains would present nine longer branches participating in the corona.

6. Conclusion

Topological grafts as the ones provided by grafted cyclodextrin−PEO complexes allow for a new class of materials, where the connection between the different elements composing the material is defined by simple topological rules.

One of the most important new features of the SGP layers that we considered here is that the sliding chains can adapt to external conditions. In the mushroom regime, where chains are only sparsely grafted to the surface, the two arms adopt mainly symmetric conformations. We exactly showed this for ideal chains and checked that it remains true for chains with excluded volume statistics. In the latter case, excluded volume correlations only slightly increase the probability of dissymmetric configurations. In these SGP systems, external forces selectively applied to one end can easily favor dissymmetric configurations. In densely grafted layers, in contrast, the chains adopt very asymmetric configurations to accommodate the strong interchain excluded volume interactions. This is merely because the free energy density of a layer of equal chains increases linearly with chain length but super linearly with grafting density. Qualitatively, a typical graft comprises a long branch and a short one filling one correlation volume (*blob*) at the surface. As the density decreases and the mushroom regime is approached, the two branches become typically comparable in size, and the size distribution is no longer bimodal. We showed also that a comparable behavior can be obtained for SGP layers grafted onto curved surfaces, with perhaps more adaptability due to the extra available space around the surface. In particular, this leads to an intermediate grafting density regime where symmetric and asymmetric chain configurations coexist.

We believe that SGP layers represent a completely new type of interfacial polymer structures and, as such, open many new possibilities that we have barely considered here. For instance, we expect the steric forces between SGP layers to be qualitatively different from the usual steric repulsion between grafted polymer layers. We hope to address this and other related questions in future extensions of our work.

References and Notes

(1) Nakashima, N.; Kawabuchi, A.; Murakami, H. *J. Inc. Phenom. Mol. Rec. Chem.* **1998**, *32*, 363−373.
(2) Ogino, H. *J. Am. Chem. Soc.* **1981,** *103*, 1303.
(3) Ogino, H.; Ohata, K. *Inorg. Chem.* **1984**, *23*, 3312.
(4) de Gennes, P.-G. *Physica A* **1999**, *271*, 231−237.
(5) Cacialli, F.; Wilson, J. S.; Michels, J. J.; Daniel, C.; Silva, C.; Friend, R. H.; Severin, N.; Samorl, P.; Rabe, J. P.; O'connell, M. J.; Taylor, P. N.; Anderson, H. L. *Nat. Mater.* **2002**, *1*, 160.
(6) Ballardini, R.; Balzani, V.; Credi, A.; Gandolfi, M. T.; Venturi, M. *Acc. Chem. Res.* **2001**, *34*, 445−455.
(7) Harada, A. *Acc. Chem. Res.* **2001**, *34*, 456−464.
(8) Schalley, C. A.; Beizai, K.; Gtle, F. V. *Acc. Chem. Res.* **2001**, *34*, 465−476.
(9) Tamura, M.; Gao, D.; Ueno, A. *Chem. Eur. J.* **2001**, 7, 1390−1397.
(10) Harada, A. *Coord. Chem. Rev.* **1996**, *148*, 115−133.
(11) Wei, M.; Shin, I. D.; Urban, B.; Tonelli, A. E. *J. Polym. Sci., Part B: Polym. Phys.* **2004**, *42*, 1369−1378.
(12) Rekharsky, M. V.; Inoue, Y. *Chem. Rev.* **1998**, *98*, 1875−1917.
(13) Heddarimane, S. M.; Fleury, G.; Schlatter, G.; Brochon, C.; Hadziioannou, G.; Marques, C. M. preprint.
(14) Fleer, G. J.; Stuart, M. C.; Scheutjens, J.; Cosgrove, T.; Vincent, B. *Polymers at Interfaces*; Chapman and Hall: London, 1993.
(15) Lipowsky, R.; Sackmann, E. *Structure and Dynamics of Membranes*; Elsevier: Amsterdam, 1995.
(16) Alexander, S. *J. Phys. (France)* **1977**, *38*, 983−987.
(17) de Gennes, P.-G. *Scaling Concepts in Polymer Physics*, 2nd ed.; Cornell University Press: Ithaca and London, 1985.
(18) Halperin, A.; Tirrell, M.; Lodge, T. P. *Adv. Polym. Sci.* **1992**, *100*, 31.
(19) Milner, S. T.; Witten, T. A.; Cates, M. E. *Macromolecules* **1989**, *22*, 853−861.
(20) Auroy, P.; Auvray, L.; Leger, L. *Phys. Rev. Lett.* **1991**, *66*, 719.
(21) Doi, M.; Edwards, S. F. *The theory of polymer dynamics*; Clarendon Press: Oxford, 1986.
(22) The image of eq 7 in the Laplace space yields $\tilde{Z}(s) \sim (1/s)\Pi_{k=2}^{m}(1/\beta_{k-1}{}^{3}) \exp[-\beta_{k-1}\sqrt{s}] (1 + \beta_{k-1}\sqrt{s})$. Applying the equality $\lim_{N\to\infty}Z = \lim_{s\to 0}s\tilde{Z}(s)$, we obtain eq 8.
(23) Abramowitz, M.; Stegun, I. A. *Handbook of mathematical functions;* National Bureau of Standards: Washington, DC, 1964.
(24) The image of eq 20 in the Laplace space is $\tilde{P}(s) = 1/(swS_0)$. Combining this expression with the image of eq 18 $\tilde{S}(s) = S_0\tilde{P}(s)/s$ and applying the inverse Laplace transform, we get eq 21.
(25) Duplantier, B. *J. Stat. Phys.* **1989**, *54*, 581−680.
(26) Johner, A.; Joanny, J.-F.; Orrite, S. D.; Avalos, J. B. *Europhys. Lett.* **2001**, *56*, 549.
(27) Daoud, M.; Cotton, J. P. *J. Phys. (France)* **1982**, *43*, 531.